



**Effects of Weight and Center of Gravity
Location of Head-Supported Devices
on Neck Loading
(Reprint)**

By

**Hashem Ashrafiun
Nabih M. Alem
B. Joseph McEntire**

Aircrew Protection Division

February 1998

Approved for public release, distribution unlimited.

**U.S. Army Aeromedical Research Laboratory
Fort Rucker, Alabama 36362-0577**

Notice

Qualified requesters

Qualified requesters may obtain copies from the Defense Technical Information Center (DTIC), Cameron Station, Alexandria, Virginia 22314. Orders will be expedited if placed through the librarian or other person designated to request documents from DTIC.

Change of address

Organizations receiving reports from the U.S. Army Aeromedical Research Laboratory on automatic mailing lists should confirm correct address when corresponding about laboratory reports.

Disposition

Destroy this document when it is no longer needed. Do not return it to the originator.

Disclaimer

The views, opinions, and/or findings contained in this report are those of the author(s) and should not be construed as an official Department of the Army position, policy, or decision, unless so designated by other official documentation. Citation of trade names in this report does not constitute an official Department of the Army endorsement or approval of the use of such commercial items.

Reviewed:

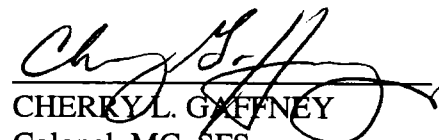


JOHN P. ALBANO
MAJ, MC, SFS
Director, Aircrew Protection
Division

Released for publication:



JOHN A. CALDWELL, Ph.D.
Chairman, Scientific Review
Committee



CHERRY L. GAFFNEY
Colonel, MC, SFS
Commanding

REPORT DOCUMENTATION PAGE

Form Approved
OMB No. 0704-0188

1a. REPORT SECURITY CLASSIFICATION Unclassified		1b. RESTRICTIVE MARKINGS	
2a. SECURITY CLASSIFICATION AUTHORITY		3. DISTRIBUTION / AVAILABILITY OF REPORT Approved for public release; distribution unlimited	
2b. DECLASSIFICATION / DOWNGRADING SCHEDULE		5. MONITORING ORGANIZATION REPORT NUMBER(S)	
4. PERFORMING ORGANIZATION REPORT NUMBER(S) USAARL Report No. 98-20		7a. NAME OF MONITORING ORGANIZATION U.S. Army Medical Research and Materiel Command	
6a. NAME OF PERFORMING ORGANIZATION U.S. Army Aeromedical Research Laboratory	6b. OFFICE SYMBOL (If applicable) MCMR-UAD	7b. ADDRESS (City, State, and ZIP Code) 504 Scott Street Fort Detrick, MD 21702-5012	
6c. ADDRESS (City, State, and ZIP Code) P.O. Box 620577 Fort Rucker, AL 36362-0577		9. PROCUREMENT INSTRUMENT IDENTIFICATION NUMBER	
8a. NAME OF FUNDING / SPONSORING ORGANIZATION	8b. OFFICE SYMBOL (If applicable)	10. SOURCE OF FUNDING NUMBERS	
8c. ADDRESS (City, State, and ZIP Code)		PROGRAM ELEMENT NO. 62787A	PROJECT NO. 30162787A878
		TASK NO. EB	WORK UNIT ACCESSION NO. DA320693
11. TITLE (Include Security Classification) (U) Effects of weight and center of gravity location of head-supported devices on neck loading (Reprint)			
12. PERSONAL AUTHOR(S) Hashem Ashrafiuon, Nabih M. Alem, and B. Joseph McEntire			
13a. TYPE OF REPORT Final	13b. TIME COVERED FROM TO	14. DATE OF REPORT (Year, Month, Day) 1998 February	15. PAGE COUNT 11
16. SUPPLEMENTAL NOTATION Originally published in Aviation, Space, and Environmental Medicine, Vol. 68, No. 10, October 1997			
17. COSATI CODES		18. SUBJECT TERMS (Continue on reverse if necessary and identify by block number)	
FIELD	GROUP	simulations, head-supported devices, crash simulation	
	SUB-GROUP		
19. ABSTRACT (Continue on reverse if necessary and identify by block number) A comprehensive study of the effect of head-supported devices (HSDs) on neck loading during helicopter accidents is presented. The new Articulated Total Body (ATB) model which treats the neck as a deformable segment was used for crash simulation. Different categories of human and manikin subjects were considered under several crash scenarios. Simulations were theoretically designed to include a wide range of HSDs by changing their weights and center of gravity (CG) locations relative to the head, and studying the effects of these changes. Since HSDs were only theoretically included in the model, detachment of specific detachable devices used in most military applications was not modeled in the study. Hence, two typical detachable devices were modeled, and selected simulations were repeated and compared not only to provide a measure of accuracy for the original results, but also to see the effect of separation of these devices from the helmet.			
20. DISTRIBUTION / AVAILABILITY OF ABSTRACT <input checked="" type="checkbox"/> UNCLASSIFIED/UNLIMITED <input type="checkbox"/> SAME AS RPT. <input type="checkbox"/> DTIC USERS		21. ABSTRACT SECURITY CLASSIFICATION Unclassified	
22a. NAME OF RESPONSIBLE INDIVIDUAL Chief, Science Support Center		22b. TELEPHONE (Include Area Code) (334) 255-6907	22c. OFFICE SYMBOL MCMR-UAX-SS

Effects of Weight and Center of Gravity Location of Head-Supported Devices on Neck Loading

HASHEM ASHRAFIUON, M.S., Ph.D., NABIH M. ALEM, M.S., Ph.D., and B. JOSEPH McENTIRE, B.S., M.S.

ASHRAFIUON H, ALEM NM, McENTIRE BJ. *Effects of weight and center of gravity location of head-supported devices on neck loading.* *Aviat Space Environ Med* 1997; 68:915-22.

A comprehensive study of the effect of Head-Supported Devices (HSDs) on neck loading during helicopter accidents is presented. The new Articulated Total Body (ATB) model which treats the neck as a deformable segment was used for crash simulation. Different categories of human and manikin subjects were considered under several crash scenarios. Simulations were theoretically designed to include a wide range of HSDs by changing their weights and center of gravity (CG) locations relative to the head, and studying the effects of these changes. Since HSDs were only theoretically included in the model, detachment of specific detachable devices used in most military applications was not modeled in the study. Hence, two typical detachable devices were modeled and selected simulations were repeated and compared not only to provide a measure of accuracy for the original results but also to see the effect of separation of these devices from the helmet.

WHILE HELMETS CONSIDERABLY reduce the risk of head injury to the crew in accidents involving helicopters and other vehicles, they normally increase the risk of injury to the neck. Further, in military applications where the use of other (usually detachable) devices such as night vision goggles (NVG) are required, neck injury may become critical. The purpose of this study is to show the effect of using Head-Supported Devices (HSDs; e.g., helmets and detachable devices) on neck loading. The study focuses on how much the maximum forces and moments acting on the neck during typical helicopter accidents are increased due to the HSD weight and center of gravity (CG) location relative to the head.

The Articulated Total Body (ATB) model (4) was used to predict the type and magnitude of loading applied to the neck through the occipital condyle (also called the head pivot) and the neck pivot during the deceleration periods of several Apache helicopter crash scenarios. The original ATB model treats segments as rigid bodies. This assumption may result in significant simulation error particularly in the head-neck response since the neck undergoes large deformation in most crashes. Recently, a new option has been added to the ATB which is capable of modeling the neck as a deformable body (1). To use this option, finite element models of the subject necks are developed to calculate their relevant vibrational mode shapes. Neck deformation is then represented by a linear combination of the mode shapes where the contribution of each mode is calculated by the ATB model based on the given environment.

The human/manikin subjects were modeled as 17 segments connected with 16 joints, as shown in Fig. 1 (segment 20 and joint j_{19} are described later). The inertial reference frame was selected such that $+x$ is forward, $+y$ is lateral pointing from left to right shoulder, and $+z$ is vertical pointing downward. All joints are of ball and socket type (free joints) except for knees and elbows (j_6, j_9, j_{12}, j_{14}) which are pin joints. The objective of the ATB simulations was to determine the reaction forces and moments at the head-neck pivots (joints j_4 and j_3). Segment and joint physical properties for different subjects were developed using the (GEBOD) program (2). There is also a vertical slip joint between the helicopter and the seat which were modeled as segments 18 and 19.

The Apache helicopter gunner seat was considered for the simulations. The seat is connected to the helicopter structure through a spring-damper system which can handle up to 15,900 N. The helicopter was modeled as a vehicle where the deceleration data corresponding to the impact condition was applied. A harness-belt system with four individual belts were defined. All belts converge to the same point on the front surface of the lower torso (segment 1). There are two shoulder belts, one waist belt wrapped around the lower torso, and a short belt from front of the seat pan to the convergence point on the lower torso.

In our study, Apache helicopter crashes carrying a manikin or a human subject were simulated. In order to do a thorough investigation, several impact conditions and a variety of subjects wearing almost any conceivable types of HSDs have been considered. Variations in HSDs were introduced through changes in their weight and CG location. Separation of detachable devices, however, was not modeled in these simulations.

Since in most Apache helicopter crashes devices detach from the helmets, the ATB software was further revised to model detachable devices for more accurate simula-

From the U.S. Army Aeromedical Research Laboratory, Fort Rucker, AL.

This manuscript was received for review in November 1996. It was revised in February 1997 and accepted for publication in May 1997.

Address reprint requests to: Dr. Hashem Ashrafiuon, who is an Associate Professor, Department of Mechanical Engineering, Villanova University, Villanova, PA 19085-1681.

Reprint & Copyright © by Aerospace Medical Association, Alexandria, VA.

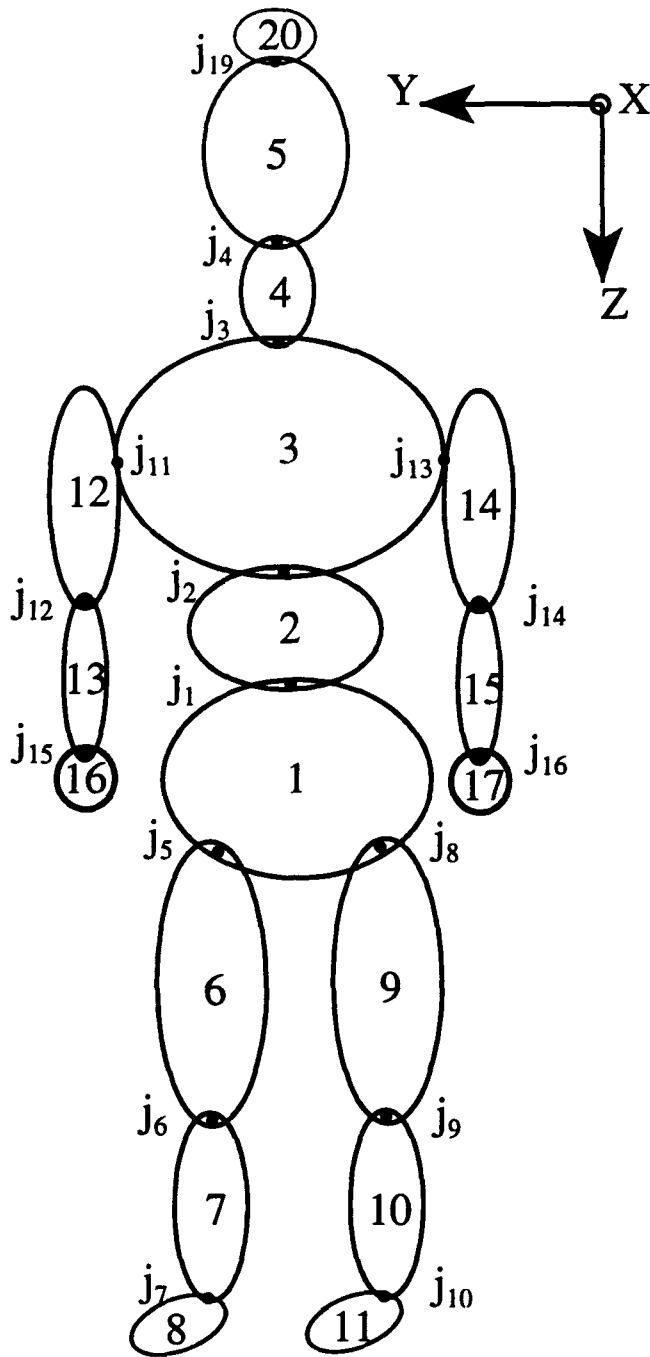


Fig. 1. The ATB 17-segment human model with a detachable device.

tions. Two helmets with detachable devices were selected: an Integrated Helmet And Display Sighting System (IHADSS) with a detachable Helmet Display Unit (HDU); and a Sound Protective Helmet number 4B (SPH-4B) with detachable Night Vision Goggles (NVG). The helmet and head were modeled as a single segment. The detachable device in each case was modeled as segment number 20 connected to the head with pin joint j_{19} (see Fig. 1). The simulations were performed with and without detachment modeling. The comparison of the time history plots of the forces and moments acting on the occipital condyle and neck pivot provided a measure of accuracy for the original simulation results where de-

tachment was not modeled. It also showed the effects of separation of detachable devices from the helmet on neck loading and subsequently neck injury.

Neck Models

The Hybrid III neck is segmented with three aluminum plates, 86.4 mm in diameter, between Butyl rubber sections to simulate the human vertebral disks. The center rubber sections have a 68.6 mm diameter. They are offset 5.1 mm towards the front of the neck and have slits to provide a different response in flexion than in extension bending. There are also aluminum end plates to facilitate assembly with a manikin. The total length of the neck is 144 mm. The material properties used are Young's Modulus, density, and Poisson's ratio which are respectively 69×10^9 Pa, $2715 \text{ kg} \cdot \text{m}^{-3}$, and 0.33 for aluminum and 8.27×10^6 Pa, $949 \text{ kg} \cdot \text{m}^{-3}$, and 0.49 for Butyl rubber.

The finite element model of the Hybrid III contains 3427 nodes and 2386 elements. The first two modes of the Hybrid III neck are excited at frequencies of 36.1 Hz and 36.3 Hz which are similar to the first bending modes of a cantilever beam. Only these first two modes are considered for the ATB simulations. Detailed data about the model can be obtained from a previous study (1).

The three human necks are simply modeled as solid cylinders with approximate Butyl rubber elastic properties (10.34×10^6 Pa for male and 8.27×10^6 Pa for female subjects) and Aluminum mass density ($2715 \text{ kg} \cdot \text{m}^{-3}$). Neck lengths are 97.5 mm, 97.5 mm, and 88.9 mm and neck radii are 35.2 mm, 39.1 mm, and 29.1 mm for the

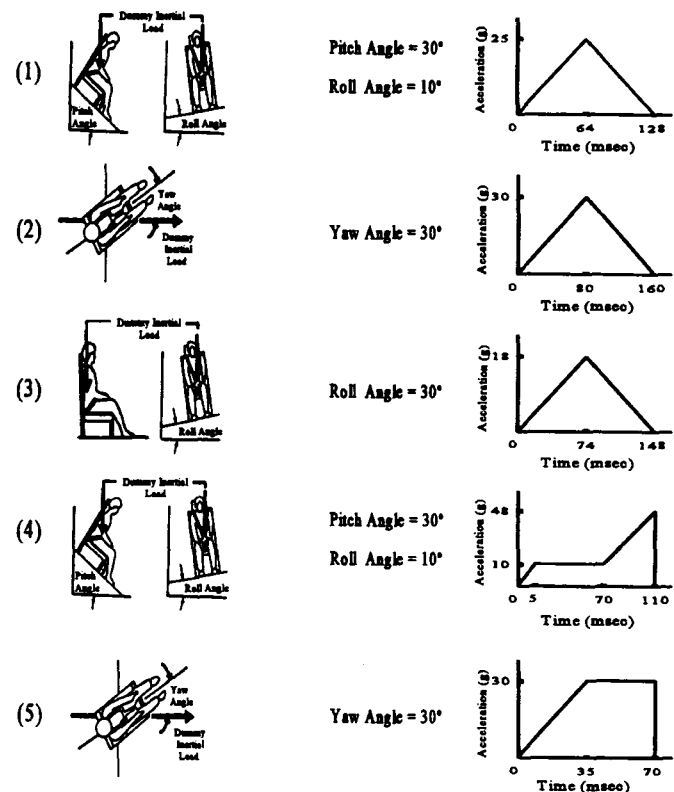


Fig. 2. The five impact conditions (pulses) selected for ATB simulations.

TABLE I. DISTRIBUTION OF HSD CENTER OF GRAVITY LOCATIONS RELATIVE TO THE HEAD CENTER OF GRAVITY IN MM.

Run Number	x	y	z
1	+40	0	0
2	+40	0	+30
3	+20	0	0
4	+20	0	+30
5	+20	0	-30
6	+20	+30	+30
7	+20	+30	-30
8	+20	-30	+30
9	+20	-30	-30
10	0	0	0
11	0	0	+30
12	0	0	-30
13	0	+30	+30
14	0	+30	-30
15	0	-30	+30
16	0	-30	-30
17	-20	0	0
18	-20	0	+30
19	-20	0	-30
20	-20	+30	+30
21	-20	-30	-30
22	-40	0	0
23	-40	0	+30
24	-40	0	-30
25	-40	+30	0
26	-40	-30	0

medium male, large male, and small female subjects, respectively. The finite element mesh of all three neck models contain 783 nodes and 592 elements. The data was validated by comparing the simulations with the experimental results obtained by the Naval Biodynamic Laboratory.

Only the first four modes are considered for the ATB simulations. The first two modes are bending modes similar to those of a beam. The third mode is a torsion mode and the fourth one is an axial tension mode. The bending modes are excited at 54.08 Hz, 57.63 Hz, and 49.85 Hz; the torsion modes at 90.42 Hz, 90.42 Hz, and 88.74 Hz; and the axial tension mode at 166.60 Hz, 166.83 Hz and 163.27 Hz for the medium male, large male, and small female subjects, respectively.

Simulations

A 50% Hybrid III manikin (3) and three human subjects representing a wide spectrum of people were selected for ATB simulations. The GEBOD program (2) was used to generate the segment and joint data for a sitting Hybrid III dummy, a 1.727 m - 756 N medium male, a 1.854 m - 979 N large male, and a 1.6 m - 534 N small female.

Five impact conditions were considered which are

TABLE III. CENTER OF GRAVITY LOCATIONS OF HSDS RELATIVE TO THE HEAD CENTER OF GRAVITY IN MM.

Type	x	y	z
IHADSS	24.2	7.2	42.8
IHADSS + HDU	22.0	-2.6	13.5
SPH-4B	14.7	8.4	-43.9
NVG	203.2	0	-12.7

shown in Fig. 2. The first one was a 25 g vertical triangular pulse of 128 ms duration with 30° pitch and 10° roll subject orientation. The second condition was a 30 g horizontal triangular pulse of 160 ms duration with 30° yaw subject orientation. The third one was an 18 g vertical triangular pulse of 148 ms duration with 30° roll subject orientation. The fourth one was a 10-48 g vertical bi-level pulse of 110 ms total duration with 30° pitch and 10° roll subject orientation. Finally, the fifth condition was a 30 g horizontal trapezoidal pulse of 70 ms total duration with 30° yaw subject orientation.

Simulations were performed with no added HSD and with the addition of four HSD weights of 4.45, 13.34, 26.69 and 40.03 N (1, 3, 6, 9 lbs). For each added HSD weight 26 different HSD CG locations were considered. The CG locations are distributed relative to the head ranging from -40 mm to +40 mm forward, -30 mm to +30 mm lateral, and -30 mm to +30 mm vertical, as listed in Table I.

Considering all possible cases, a total of 2100 ATB simulations have been performed. There were 26 cases based on CG locations per added HSD weight plus the case with no HSD making up 105 cases per impact condition per subject. In each case, the maximum forces and moments acting on the head and neck pivots were calculated. The components of the forces and moments are expressed in the neck coordinate system which was initially assumed to be parallel to the inertial reference frame; i.e., z-axis of the neck is pointing from j_4 down to j_3 joint.

To investigate the effect of detachment, a total of 40 simulations were performed twice, once assuming that segment 20 (HDU or NVG) can not detach and another where it is detachable. The 40 simulations represent 5 impact conditions for 4 subjects first wearing the IHADSS helmet with HDU and the second time wearing the SPH-4B helmet with NVG. The comparison showed the effect of separation of detachable devices and provided a measure of accuracy for the original 2100 simulations where detachment was not modeled.

Head-Supported Devices

Two HSDs were selected for this study: an IHADSS with a detachable HDU; and a SPH-4B with detachable

TABLE II. INERTIA PROPERTIES OF THE SELECTED HSDS IN NEWTONS AND $\text{KG} \cdot \text{M}^2 \times 10^{-4}$.

Type	Weight	I_{xx}	I_{yy}	I_{zz}	I'_{xy}	I'_{xz}	I'_{yz}
IHADSS	14.407	192.85	153.26	199.70	209.19	219.23	196.22
IHADSS + HDU	17.925	320.19	256.72	243.83	296.73	300.12	252.90
SPH-4B	13.598	166.44	161.05	172.09	163.54	179.17	154.21
NVG	5.146	6.44	5.18	8.78	—	—	—

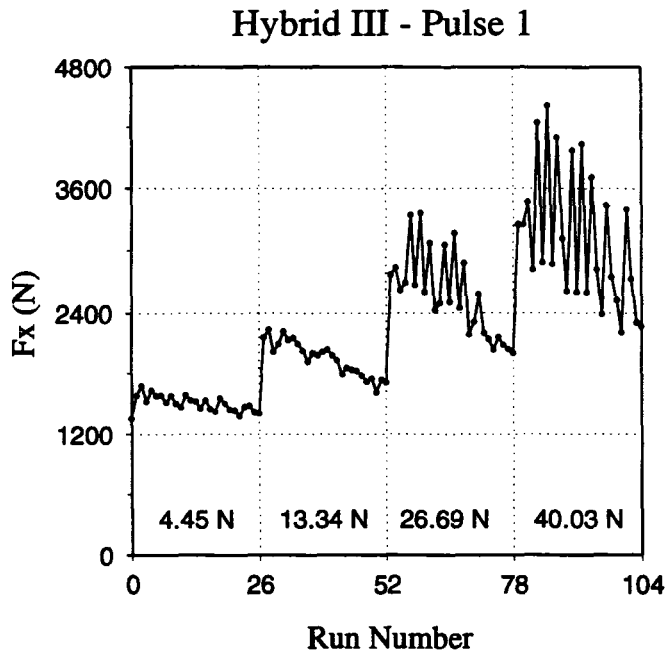


Fig. 3. Maximum forces along the neck x-axis at the head pivot joint.

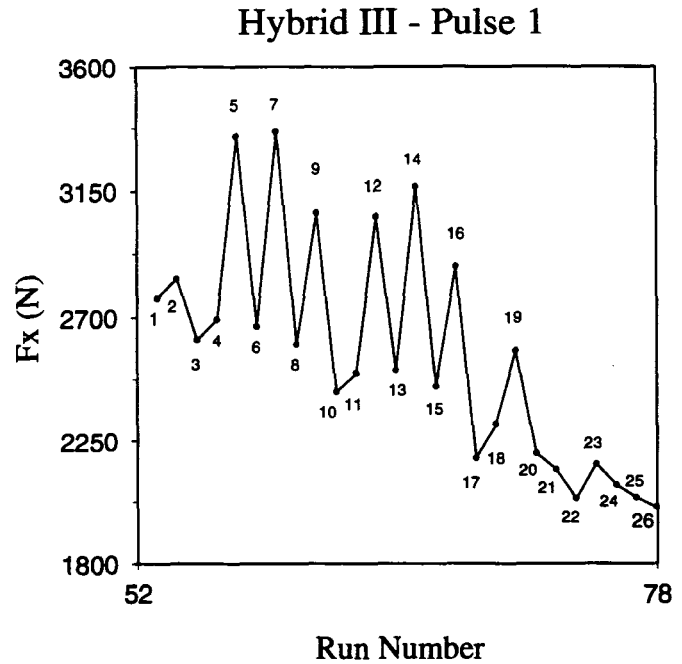


Fig. 4. The portion of figure 3 corresponding to a 26.69-N HSD.

NVG. The moments and products of inertia of the selected HSDs were measured with respect to the helmet CG and in a reference frame that is rotated 180° about the x-axis of the ATB inertial reference frame such that z is upward and y points from right to left shoulder. Hence, the products of inertia used in the inertia matrix can be calculated from the measured inertias using the following equations:

$$I_{xy} = \frac{I_{xx} + I_{yy}}{2} - I'_{xy} \quad \text{Eq. 1}$$

$$I_{xz} = \frac{I_{xx} + I_{zz}}{2} - I'_{xz} \quad \text{Eq. 2}$$

$$I_{yz} = \frac{I_{yy} + I_{zz}}{2} - I'_{yz} \quad \text{Eq. 3}$$

where I'_{xy} , I'_{xz} , and I'_{yz} are the measured values.

The helmet and the head inertia properties were transformed to the ATB coordinate system and combined such that they can be modeled as a single segment. The helmet inertia matrix was simply rotated 180° about ATB's x-axis and the head principal inertias were transformed using principal axes rotation given in the GEBOD generated data files. Inertia properties of the combined segment were then calculated using the parallel axis theorem. However, the inertia properties of detachable devices were calculated so that they can be modeled as individual segments.

IHADSS helmet with HDU: An extra large size IHADSS helmet with its visor down was used in this study. The mass and geometric properties were measured with and without the HDU which are listed in Table II. The CG locations of the helmet with respect to the head are listed in Table III. Given the data shown in Tables II and III, the inertia matrix and CG location of the HDU can be calculated.

The HDU is connected to IHADSS through a pin joint

located approximately at 0, 127 mm, 76.2 mm relative to the head CG coordinate system. The pin axis is parallel to the head x-axis. The HDU will be detached when the joint moment about the joint axis exceeds +2.0 N.m (ccw).

SPH-4B helmet with night vision goggles: An extra large size SPH-4B helmet with its visor up was also used in this study. The mass and geometric properties of the SPH-4B and NVG were measured and are listed in Table II. The products of inertia are zero due to nearly symmetric geometry. The CG locations of the helmet and NVGs with respect to the head are shown in Table III.

NVG is connected to SPH-4B through a pin joint located approximately 203.2 mm, 0, -43.2 mm relative to the head CG coordinate system. The pin axis is parallel to the head (and NVG) y-axis. The NVG will be detached under three different conditions: a) when the joint force in the head x-z plane pointing toward positive x (first and fourth quadrants) exceeds 57.8 N; b) when the joint moment about the axis parallel to the head z-axis exceeds 1.5 N.m; and c) when the joint moment about the joint axis exceeds -1.2 N.m (cw).

RESULTS

All extreme values of the forces and moments acting on the occipital condyle and the neck pivot along the positive and negative principal axes of the neck were collected and plotted in groups of 105 values per pulse per subject. For example, Fig. 3 shows a typical graph where, in this case, the maximum values of the reaction force acting at joint j_4 of the Hybrid III opposite the neck x-axis (reacting to forward head motion) are plotted.

Run number 0 in Fig. 3 represents the case with no HSD, run numbers 1-26 represent the values obtained from simulations with a 4.45 N (1-lb) HSD corresponding to the 26 CG locations listed in Table I. Similarly, run

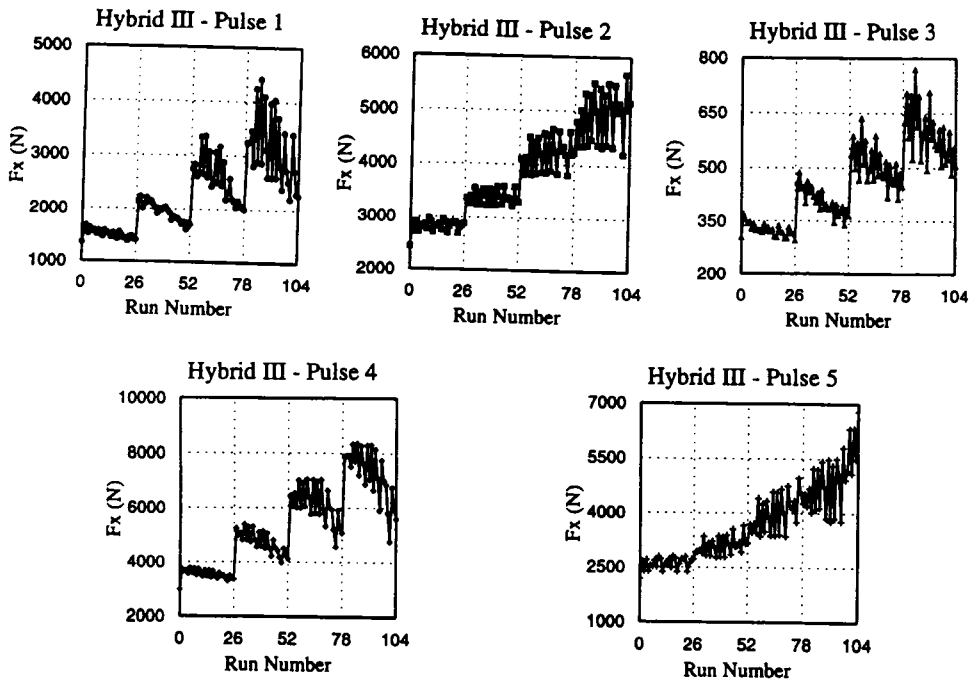


Fig. 5. Maximum x-force at the head pivot joint of the Hybrid III.

numbers 27–52, 53–78, and 79–104 represent the values obtained from simulations with 13.34-N (3-lb), 26.69-N (6-lb), and 40.03-N (9-lb) HSDs corresponding to the 26 CG locations listed in Table I. In order to clearly distinguish values corresponding to each of the 26 CG locations, Fig. 4 shows the portion of Fig. 3 corresponding to the 26.69-N HSD where the CG locations are numbered according to the listing in Table I.

All 2100 simulations were performed and the results have been plotted. Since for most of the simulations only the $-x$ and $+z$ components of the force and $+y$ component of the moment at the occipital condyle (j_4) and neck pivots (j_3) are relevant, other components have been ignored. The five graphs obtained from responses to the

five impact conditions were then grouped together in a single figure. Fig. 5 shows the maximum forces at the occipital condyle in the neck $-x$ direction for the Hybrid III dummy subjected to the five impact conditions. Fig. 6 shows the maximum moments at the neck pivot about the neck $+z$ direction for the large male subjected to the five impact conditions. Figs. 7 and 8 show the same maximum forces and moments for the small female and medium male subjects, respectively.

It can be seen clearly in Figs. 5–8 that the maximum forces and moments acting on the neck significantly increase every time HSD weights are raised; i.e., steps 1, 27, 53, and 79. It can also be stated that the maximum forces and moments are generally decreased as the HSD

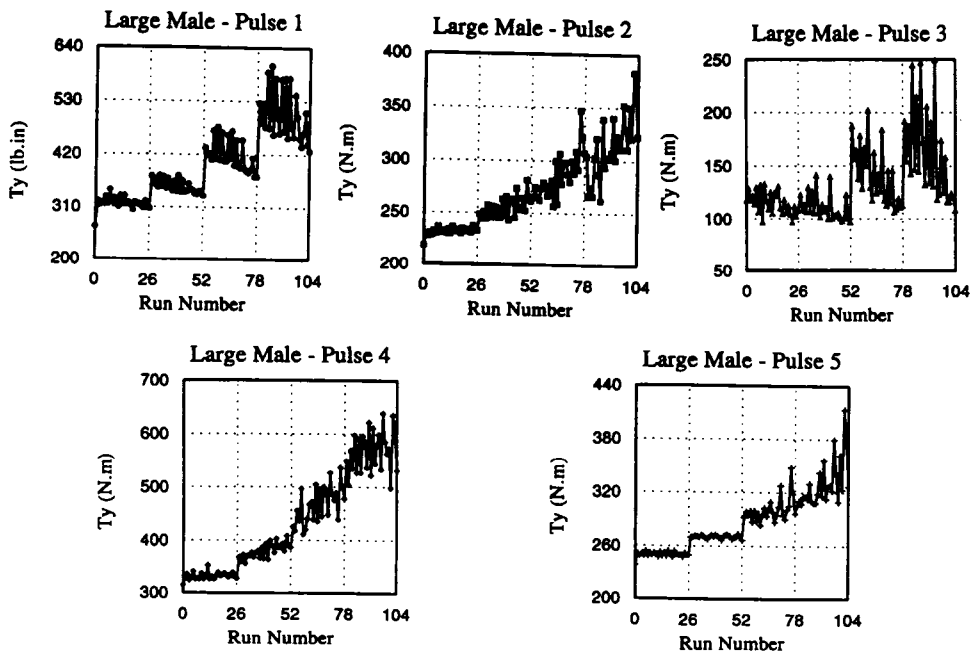


Fig. 6. Maximum y-torque at the neck pivot joint of the large male.

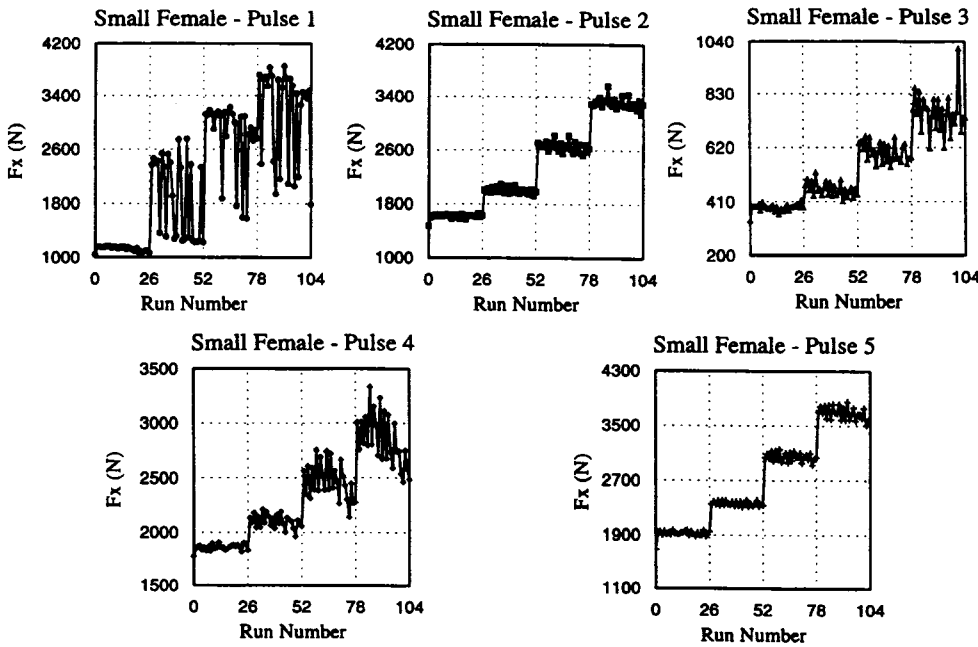


Fig. 7. Maximum x-force at the occipital condyle the small female.

CG is moved downward (toward +z). This can be seen clearly in Fig. 4, where cases 5, 7, 9, 12, 14, 16, and 19 have higher forces and correspond to $z = -30$ mm. Further, cases 4, 6, 8, 11, 13, 15, and 18 have lower forces and correspond to $z = +30$ mm and most of the remaining cases, where the forces fall in between, correspond to $z = 0$. Similar patterns can be detected in other subjects and impact conditions, though not consistently, as shown in Figs. 5–8.

The variation of HSD CG in x seem to have different effects based on the impact. Since the cases are ordered from + to - x values (Table I), the effect of variations in x direction can be observed through the slope of the linear least square fit of the graph of each HSD weight separately. When the subjects are simulated under verti-

cal impact conditions (pulses 1, 3–4), the maximum neck forces and moments decrease as the HSD CG is moved backward except in a few cases where the change is insignificant (Figs. 5–8). However, under horizontal impact conditions (pulses 2, 5), the maximum moments increase while the maximum forces decrease, as the HSD CG is moved backward. Thus, it may only be stated that under vertical impact conditions, the neck forces and moments are generally decreased as the HSD CG is moved backward (-x).

There can not be any general conclusions about the CG location variation in the y (lateral) directions. However, there are some cases where a lateral offset in the HSD CG could cause a significant increase in neck loading. This can be observed in Fig. 8 where the maximum

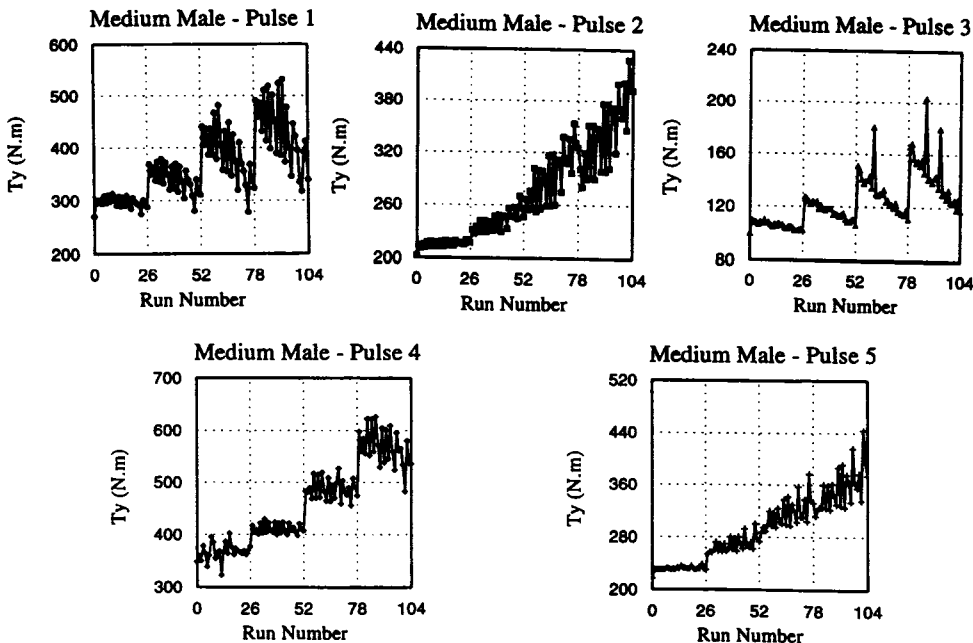


Fig. 8. Maximum y-torque at the neck pivot joint of the medium male.

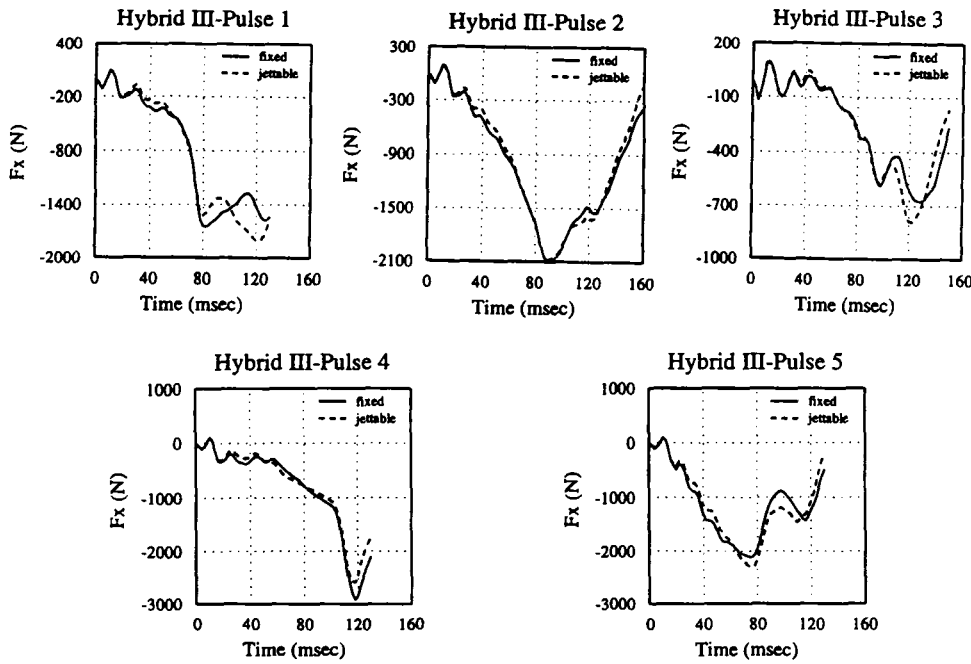


Fig. 9. Comparison of head pivot x-force for the Hybrid III with IHADSS and HDU.

neck pivot moment shows three exceptionally high peaks when the medium male is subjected to pulse 3. These peaks correspond to cases 9 and 16 for the 40.03-N HSD and case 9 for the 26.69-N HSD where the CG is moved upward and to the left of the subject at the same time (in case 9 moved forward also). Note that the pulse is downward and from left to right of the subject (due the 30° roll) such that lateral adjustment of HSD CG will not be symmetric.

Separation of detachable devices has been incorporated in the ATB model and some samples of its effects are shown in Figs. 9 and 10. Fig. 9 shows the force acting at joint j_4 along the neck x-axis for the Hybrid III dummy wearing an IHADSS helmet with HDU. Fig. 10 shows

the same for the small female subject wearing a SPH-4B helmet with NVG. All figures show that detachment occurs under all impact conditions and that it may reduce or increase the forces acting on the neck up to 10%. This implies there may be up to 10% error in the simulation results presented earlier. Simulation times at which detachment of each device occurs are listed in Table IV for the four subjects under the five impact conditions.

Finally, there is an interesting observation as a result of this study regarding how well the Hybrid III neck represents the human neck since it responds very differently to all impact conditions compared with the human subjects. The maximum forces and moments under most impact are much higher for the Hybrid III than those

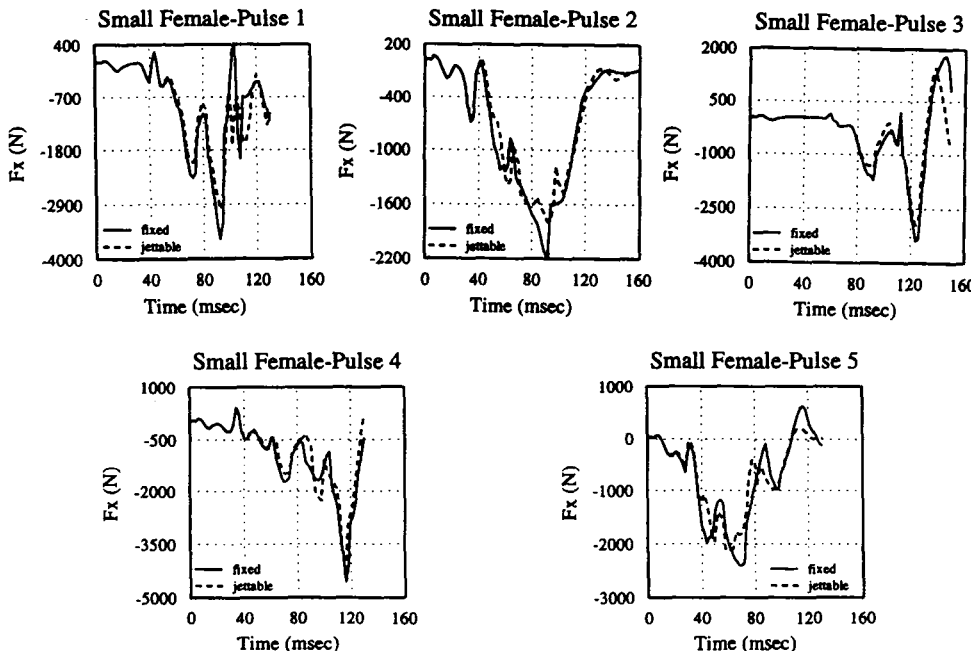


Fig. 10. Comparison of occipital condyle x-force for the small female with SPH-4B and NVG.

TABLE IV. DETACHMENT TIMES DURING THE FIVE IMPACT CONDITIONS IN MS.

	Impact Number				
	1	2	3	4	5
IHADSS + HDU					
Hybrid III	11	11	11	11	11
Medium Male	83	89	81	75	73
Large Male	85	97	93	75	79
Small Female	13	13	13	13	13
SPH-4B + NVG					
Hybrid III	29	27	71	23	15
Medium Male	37	27	63	17	15
Large Male	23	21	63	29	17
Small Female	39	31	73	29	15

shown for the human subjects; e.g., compare Figs. 5 and 7.

CONCLUSIONS

The effect of head supported devices on the human and manikin necks during several different types of helicopter crash scenarios has been investigated. A wide range of HSDs were considered by theoretically changing their weight and CG locations relative to the head.

Several conclusions have been achieved through a simple preliminary study. First, the addition of HSD weights proportionally adds to neck loading. Second, neck forces and moments are generally decreased as the HSD CG is moved downward and backward relative to the head. Third, lateral adjustment of the HSD CG could result in significantly higher forces under certain conditions. Also, to gain confidence in the results, detachment of two specific detachable devices were simulated and shown to cause a reduction or increase of up to 10% in neck forces/moments. Hence, it is recommended, though further research is needed, to design HSDs such that they are light and their CG locations are somewhat toward the lower back of the head but laterally central.

REFERENCES

1. Ashrafiuon H, Colbert R, Obergefell LA, Kaleps I. Modeling of a deformable manikin neck for multibody dynamic simulation. *Mathematical and Computer Modelling* 1996; 24:45-56.
2. Gross ME. The GEBODIII program user's guide and description. National Technical Information Service, Springfield, VA: AL-TR-1991-0102, 1991.
3. Kaleps I, White RP, Beecher RM, Whitestone J, Obergefell LA. Measurement of Hybrid III dummy properties and analytical simulation data base development. National Technical Information Service, Springfield, VA: AAMRL-TR-88-005, 1988.
4. Obergefell LA, Gardner TR, Kaleps I, Fleck JT. Articulated total body model enhancements-volume 2: user's guide. National Technical Information Service, Springfield, VA: AAMRL-TR-88-043, 1988.